Computers and Chemical Engineering 33 (2009) 1584–1592

Contents lists available at ScienceDirect

Computers and Chemical Engineering

journal homepage: www.elsevier.com/locate/compchemeng

Predictive optimal management method for the control of polygeneration systems

Andrés Collazos[a,*], François Maréchal[a], Conrad Gähler[b]

[a] École Polytechnique Fédérale de Lausanne, Laboratoire d'Énergétique Industrielle, LENI-STI, Bât. ME A2, Station 9, 1015 Lausanne, Switzerland
[b] Siemens Building Technologies Group, Zug, Switzerland

ARTICLE INFO

Article history:
Received 24 October 2008
Received in revised form 29 April 2009
Accepted 12 May 2009
Available online 21 May 2009

Keywords:
Predictive control
Optimal management
Polygeneration
Micro-cogeneration

ABSTRACT

A predictive optimal control system for micro-cogeneration in domestic applications has been developed. This system aims at integrating stochastic inhabitant behavior and meteorological conditions as well as modelling imprecisions, while defining operation strategies that maximize the efficiency of the system taking into account the performances, the storage capacities and the electricity market opportunities.

Numerical data of an average single family house has been taken as case study. The predictive optimal controller uses mixed-integer and linear programming where energy conversion and energy services models are defined as a set of linear constraints. Integer variables model the start-up and shut-down operations as well as the load dependent efficiency of the cogeneration unit. The proposed control system has been validated using more complex building and technology models to asses model inaccuracies. Typical demand profiles for stochastic factors have been used.

The system is evaluated in the perspective of its usage in Virtual Power Plants applications.

1. Introduction

The integration of polygeneration systems in urban areas is seen as one of the promising routes for adressing CO_2 mitigation problems. For example, decentralized combined heat and power production is foreseen in virtual power plant concepts (Management Summary Report of EU-Project No. NNE5-2000-208, 2005). The design of polygeneration systems in urban areas lies on the definition of the system management strategy that decides the operation of the energy conversion equipment (cogeneration and heat pumping) and of the energy storage system in order to provide the energy services required at minimum cost.

The potential benefit of cogeneration technologies for domestic applications has been assessed by numerous studies (Dorer, Weber, & Weber, 2005; Entchev et al., 2004; Pearce, Zahawi, Awckland, & Starr, 1996; Pearce, Zahawi, & Shuttleworth, 2001; Lamon, Gähler, & Gwerder, 2007; Laubacher, 2006). Some of these assessments consider the crucial question of operational control, and besides simple on–off control (Entchev et al., 2004), they may use some kind of predictive control strategy (Dorer et al., 2005; Lamon et al., 2007). However, aside from Entchev et al. (2004) that was an application on a real plant, the other works used identical models for the control strategy optimisation and the validation of the controller. Furthermore, future conditions were known in advance.

The design method is based on the definition of typical days from which the ambient temperature and the demand profiles are taken as reference. One key component of this strategy is the energy storage equipment that is used to create a time shift between the energy conversion and the demands allowing for equipment size reduction and better profitability. When the management strategy is based on optimisation methods such as those presented by Weber, Maréchal, Favrat, and Kraines (2006), the design method lies on the definition of typical days during which the performances are computed assuming a perfect knowledge of the temperature profiles and energy demand. This assumption is, however, not acceptable when implementing the management strategy for an existing system since these profiles are stochastic and are not perfectly predictable.

The goal of this paper is to present a predictive control strategy developed for the optimal management of a polygeneration system in a complex multiservices system that is installed to deliver heat, hot water and electricity to a residential building. The method includes a predictive model of the energy demand of the building based on the prediction of the ambient temperature and an Auto Regressive model with eXternal inputs (ARX) of the building heat losses, combined with a simplified simulation of the heat distribution system. The optimal management strategy uses a mixed-integer linear programming model to decide the start-up and shut-down of the equipment and manage the heat storage.

The optimal control system developed has been validated by connecting it with a detailed building simulation model that is

* Corresponding author at: Centre de Recherches en Physique des Plasmas, Association Euratom-Confédération Suisse, 1015 Lausanne, Switzerland
E-mail address: andres.collazos@epfl.ch (A. Collazos).

0098-1354/$ – see front matter © 2009 Elsevier Ltd. All rights reserved.
doi:10.1016/j.compchemeng.2009.05.009

Nomenclature

Lower indexes

b	relative to the boiler
cg	relative to the cogeneration unit
dhw	relative to the domestic hot water tank
el	relative to the electricity consumption
gas	relative to the gas consumption
h	relative to the building (house)
hs	relative to the heat storage
vlv	relative to the three-way valve

Upper indexes

$+, -$	respectively incoming and outgoing energy, heat or electricity (for disambiguation)
$*$	denotes an optimal quantity
loss	losses to the environment (variables)
max, min	maximum and minimum values (parameters)
req	requirements (parameters)

Symbols

$\alpha_1, \alpha_2, \lambda$	parameters for calculating the losses of the heat storage tanks
a_1, a_2, b_1, b_2	ARX building model parameters
$\mathbf{C}$	operating costs (euro)
c_{hour}	cost per hour of operation for maintenance (cogeneration unit) (euro/h)
$\mathbf{cg_{on}}$	indicator if the cogeneration unit is on (binary variable)
$\mathbf{cg_{pw}}$	auxiliary binary variable for piecewise cogeneration unit output
$\mathbf{cg_{start\text{-}up}}$	indicator if the cogeneration has started
$c_{\mathrm{start\text{-}up}}$	cost per start-up (cogeneration unit) (euro/start-up)
c	cost per kilowatt (euro/kW)
c_p	specific heat capacity of water (kJ/ °C kg)
$\dot{E}$	electrical flow (kW)
$\dot{H}$	fuel energy flow (kW)
$\mathbf{J}$	resulting objective function (operating costs + comfort penalty) (euro)
$m_1^{\mathrm{el}}, m_1^{\mathrm{el}}, m_1^{\mathrm{gas}}, m_2^{\mathrm{gas}}$	slopes of the electrical output and fuel consumption piecewise model
M	comfort penalty weight (euro/ °C h)
$\dot{m}$	mass flow (kg/h)
$n_{\mathrm{cg,on}}^{\min}$	minimum number of hours the cogeneration unit has to run once it has been started (h)
$\tilde{n}_{\mathrm{cg,on}}^{\min}$	minimum number of hours the cogeneration still has to stay on (from past optimisations) (h)
$\mathbf{p}_{\mathrm{inf}}, \mathbf{p}_{\mathrm{sup}}$	comfort penalties (°C)
$\dot{Q}$	heat flow (kW)
Q	stored heat (J)
R_{h}	heat loss coefficient of the building (kW/h)
t_0	initial (present) time (h)
Δt	time step between optimisations (h)
Δt_{MH}	moving horizon time length (h)
Δt_{sim}	simulation time step (h)
T	temperature (°C)
T^{ext}	external temperature (°C)
$\Delta T_0, T_0^{\mathrm{ext}}, T_0^{\min}, q$	minimum heat storage tank temperature calculation parameters (refs.: Norme SIA 384/2, 1988; Zehnder, 2004)
U	set of decision variables
$\mathbf{u}$	decision variables
V, h, D, d	volume, height, external and internal diameter of a storage tank (m^3, m)

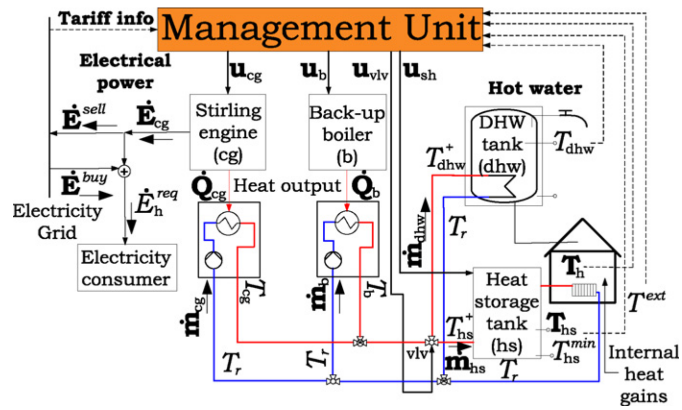

Fig. 1. Test case system studied.

assumed to represent the real non-linear and stochastic behavior of the building in its environment.

Finally, as targeted in virtual power plants concepts, it will be demonstrated that the management of the system can exploit the variable prices of the electricity market by exploiting the heat storage systems – including the building structure – to increase the combined heat and power production, therefore increasing the benefit of the system.

2. Energy system studied

The system under study, presented in Fig. 1 includes one cogeneration unit and a backup boiler, both fueled by natural gas. The system supplies energy to two heat storage tanks: one for the heating system and the other for the domestic hot water (DHW). The temperature in the heat distribution system (radiator system) is controlled by a three-way valve and the temperature set-point is determined as a function of the ambient and room temperatures using a heat loss and a heat distribution model.

In Fig. 1 T_{h} and T^{ext} are the room and outside temperatures of the building. T_{cg} is the temperature of the water exiting the cogeneration unit, T_{b} is the temperature of the water exiting the backup boiler, T_{dhw} is the temperature of the hot water going into the domestic hot water tank, T_{hs} is the temperature of the hot water going into the heat storage tank and T_{r} is the nominal return temperature of the water. $\dot{m}_{\mathrm{cg}}$ and $\dot{m}_{\mathrm{b}}$ are the mass flows entering the cogeneration unit and the backup boiler, respectively. $\dot{m}_{\mathrm{hs}}$ and $\dot{m}_{\mathrm{dhw}}$ are the mass flows sent to the heat storage and the domestic hot water tank. $\dot{E}_{\mathrm{cg}}$ is the electrical power output of the cogeneration unit, $\dot{E}_{\mathrm{el}}^{\mathrm{buy}}$ is the electrical power bought from the electricity grid, $\dot{E}_{\mathrm{el}}^{\mathrm{sell}}$ is the power sold to the grid and $\dot{E}_{\mathrm{h}}^{\mathrm{req}}$ is the electrical power consumption of the building.

The decision variables, at every time t, are the load charge of the cogeneration unit $\mathbf{u}_{\mathrm{cg}}(t) = \dot{Q}_{\mathrm{cg}}(t)/\dot{Q}_{\mathrm{cg}}^{\max}$, the load charge of the storage heat output $\mathbf{u}_{\mathrm{hs}}(t) = \dot{Q}_{\mathrm{hs}}(t)/\dot{Q}_{\mathrm{hs}}^{\max}$, the load charge of the backup boiler $\mathbf{u}_{\mathrm{b}}(t) = \dot{Q}_{\mathrm{b}}(t)/\dot{Q}_{\mathrm{b}}^{\max}$, and the three-way valve control $\mathbf{u}_{\mathrm{vlv}}(t) = \dot{Q}_{\mathrm{hs}}(t)/(\dot{Q}_{\mathrm{hs}}(t) + \dot{Q}_{\mathrm{dhw}}(t))$.

In the controller implementation, the decision variables will be translated into valve positions or temperature set points.

The building characteristics correspond to the SIA 380/1 target value single family building described by Dorer et al. (2005).

The sizes of the units in the system have been calculated using the Queuing Multi Objective Optimizer (QMOO) (Leyland, 2002) in combination with a linear programming problem as described in Weber et al. (2006). The sizes of the units considered are presented in Table 1.

Table 1
System unit characteristics. $\dot{Q}^{max}$ = maximum heat output, η = efficiency, $\dot{E}^{max}$ = maximum electrical output, η_{el} = electrical efficiency, η_{th} = thermal efficiency, V = volume.

Boiler		Cogeneration engine				Heat storage		DHW tank
$\dot{Q}_b^{max}$ [kW]	η_b	$\dot{E}_{cg}^{max}$ [kW]	$\eta_{cg,el}$	$\dot{Q}_{cg}^{max}$ [kW]	$\eta_{cg,th}$	V_{dhw} [m^3]	$\dot{Q}_{hs}^{max}$ [kW]	V_{hs} [m^3]
2.17	0.8	2.25	0.2–0.25	6.83	0.7–0.75	0.45	10	0.12

For an expected annual consumption of 8.2 MWh of space heating, 3.3 MWh of domestic hot water consumption and 2.6 MWh of electricity, the overall estimated operating costs reduction is in the order of 25%. In particular, the amount of electricity bought from the grid is 35% less for the system with a cogeneration unit.

The size of the cogeneration unit corresponds to an overall full load operating time of 3962 h per year. The variable thermal and electrical efficiencies used are based on the manufacturer's technical data (Solo Stirling, 2005).

3. The predictive controller

Several types of optimal control strategies have been developed to improve residential and non-residential building performance in terms of energy consumption: a stochastic controller to take into account significant solar gains (Nygard-Ferguson, 1990), neural networks for high thermal inertia buildings (Arigiriou, Bellas-Velidis, & Balaras, 2000), optimal control strategy for hybrid systems applied to domestic hot water production using solar energy (Prud'Homme, 2002), "soft computing" techniques for residential fuel cell energy systems optimisation (Entchev, 2003), a predictive and adaptive heating control system (Morel, Bauer, El-Khoury, & Krauss, 2001), a genetic algorithm that takes into account user wishes in an advanced control system (Guillemin, 2003) or predictive control for integrated room automation (Gwerder & Tödtli, 2005) applied to concrete core conditioning systems (Güntensperger et al., 2005), to cite a few.

For this work, a predictive control strategy that calculates the optimal values of the decision variables $\mathbf{U}(t) = (\mathbf{u}_{cg}(t), \mathbf{u}_b(t), \mathbf{u}_{hs}(t), \mathbf{u}_{vlv}(t))$ for $t = t_0, t_0 + \Delta t, \ldots, t_0 + \Delta t_{MH}$ is proposed. It aims to minimize the operating costs satisfying the comfort constraints for this period. t_0 is the time at which the strategy is calculated, and Δt_{MH} is the length of the moving horizon. The strategy is re-evaluated after every time step Δt.

To calculate these values, a Mixed Linear Integer Program (MILP), described in Eqs. (1)–(47), is solved. The objective of the MILP is to minimize the sum of the operating costs combined with a penalty term that is proportional to the time during which the room temperature does not comply with the comfort range. In order to give a priority to comfort, a significant relative weight (M) is assigned in the objective function to the comfort penalties.

The operating costs are the sum of the gas consumption in the cogeneration unit and backup boiler, added to cost of the imported and the benefit of the exported electricity. Varying electricity price is considered to take into account the possibility for the owner to access the electricity market price.

The backup boiler is modelled as a zero order model with a constant efficiency. The losses in the storage tanks are modelled using standard heat loss equations. The minimum required temperature for space heating water is calculated using the normalized equation from SIA (Société, 1988) applied to the nominal outlet temperature $T_{ext,0}$ and the nominal heating water supply temperature $T_{min,0}$ (Zehnder, 2004). The room temperature of the building is calculated by a second order ARX model with the space heating delivered as input

3.1. Mixed-integer and linear programming model

3.1.1. Objective function

$$\mathbf{U}^*(t_0) = \min_{\mathbf{U}(t)} \sum_{t=t_0}^{t_0+\Delta t_{MH}} \mathbf{J}(\mathbf{U}(t)) \tag{1}$$

where $\mathbf{U}^*(t_0) = (\mathbf{u}^*_{cg}(t_0), \mathbf{u}^*_{hs}(t_0), \mathbf{u}^*_{dhw}(t_0), \mathbf{u}^*_{vlv}(t_0))$ is the set of optimal values of the decision variables at t_0, and

$$\mathbf{J}(\mathbf{U}(t)) = \mathbf{C}_{op}(\mathbf{U}(t)) + (\mathbf{p}_{inf}(t) + \mathbf{p}_{sup}(t))\,\Delta t, \tag{2}$$

is the combined cost function subject to the operating costs, the comfort penalties and the energy model of the system studied, described in the following sections.

3.1.2. Operating costs

$$\mathbf{C}_{op}(\mathbf{U}(t)) = \mathbf{C}_{cg}(t) + \mathbf{C}_b(t) + \mathbf{C}_{el}(t), \tag{3}$$

$$\mathbf{C}_{cg}(t) = (\dot{H}_{cg}(t) \cdot c_{gas} + \mathbf{cg_{on}}(t) \cdot c_{hour})\,\Delta t + c_{start\text{-}up} \cdot \mathbf{cg_{start\text{-}up}}(t), \tag{4}$$

$$\mathbf{C}_b(t) = \dot{H}_b(t) \cdot c_{gas} \cdot \Delta t, \tag{5}$$

$$\mathbf{C}_{el}(t) = (\dot{E}_{el}^{buy}(t) \cdot c_{el}^{buy}(t) - \dot{E}_{el}^{sell}(t) \cdot c_{el}^{sell}(t))\,\Delta t, \tag{6}$$

For simplicity, the link between the costs $\mathbf{C}_{cg}$, $\mathbf{C}_b$, $\mathbf{C}_{el}$ and the decision variables in $\mathbf{U}(t)$ is not explicited.

The electricity costs c_{el}^{buy} and c_{el}^{sell} are

$$c_{el}^{buy} = \begin{cases} 0.07[\text{euro/kWh}], & \text{if } 10\,\text{p.m.} < t < 6\,\text{a.m.} \\ 0.18[\text{euro/kWh}], & \text{otherwise} \end{cases}$$

$$c_{el}^{sell} = 0.06\,\text{euro/kWh}$$

3.1.3. Comfort penalties

$$\mathbf{p}_{inf}(t) \geq M(T_h^{min}(t) - T_h(t)), \tag{7}$$

$$\mathbf{p}_{sup}(t) \geq M(T_h(t) - T_h^{max}(t)), \tag{8}$$

$$\mathbf{p}_{inf}(t), \mathbf{p}_{sup}(t) \geq 0 \tag{9}$$

$$T_h^{min}(t) = \begin{cases} 16\,^\circ\text{C}, \text{if } 11\,\text{p.m.} < t < 7\,\text{a.m.} \\ 20\,^\circ\text{C}, \text{otherwise} \end{cases} \tag{10}$$

$$T_h^{max}(t) = 21\,^\circ\text{C}. \tag{11}$$

where in Eqs. (7) and (8) M was 10^6 to make the temperature comfort a priority. In other words, the comfort penalties dominate the optimisation in case of a comfort violation, otherwise, the costs dominate, since the comfort penalties are equal zero. Note that to use a more balanced weighting, making costs and comfort penalties in the same order of magnitude, results in a broadening of the comfort range.

In Eq. (11), the maximum temperature T^{max} inside the building was introduced to avoid overheating due to free gains or extra-heating due to attractive prices on the electricity market considering that the system does not have a cooling system.

3.1.4. The system model

Backup boiler:

$$\dot{Q}_{\mathrm{b}}(t) = \mathbf{u}_{\mathrm{b}}(t)\cdot\dot{Q}_{\mathrm{b}}^{\max}, \tag{12}$$

$$\eta_{\mathrm{b}}\cdot\dot{H}_{\mathrm{b}}(t) = \dot{Q}_{\mathrm{b}}(t). \tag{13}$$

Cogeneration unit:

$$\dot{Q}_{\mathrm{cg}}(t) = \mathbf{u}_{\mathrm{cg}}(t)\cdot\dot{Q}_{\mathrm{cg}}^{\max}, \tag{14}$$

$$\begin{aligned}\dot{E}_{\mathrm{cg}}(t) = {} & \mathbf{cg_{on}}(t)\cdot\dot{E}_{\mathrm{cg}}^{\min} + \mathbf{cg_{start\text{-}up}}(t)\cdot\eta_{\mathrm{cg,el}}^{\text{start-up}}\cdot\dot{H}_{\mathrm{cg}}^{\max}\,\Delta t \\ & + \mathbf{cg_{pw}}(t)[m_1^{\mathrm{el}}(\dot{Q}_{\mathrm{cg}}(t) - \dot{Q}_{\mathrm{cg}}^{\min}) + \dot{E}_{\mathrm{cg}}^{\min}] \\ & + (1 - \mathbf{cg_{pw}}(t))[m_2^{\mathrm{el}}(\dot{Q}_{\mathrm{cg}}(t) - \dot{Q}_{\mathrm{cg,pw}}) \\ & + m_1^{\mathrm{el}}(\dot{Q}_{\mathrm{cg,pw}} - \dot{Q}_{\mathrm{cg}}^{\min})],\end{aligned} \tag{15}$$

$$\begin{aligned}\dot{H}_{\mathrm{cg}}(t) = {} & \mathbf{cg_{on}}(t)\cdot\dot{H}_{\mathrm{cg}}^{\min} + \mathbf{cg_{start\text{-}up}}(t)\cdot\dot{H}_{\mathrm{cg}}^{\max}\,\Delta t \\ & + \mathbf{cg_{pw}}(t)[m_1^{\mathrm{gas}}(\dot{Q}_{\mathrm{cg}}(t) - \dot{Q}_{\mathrm{cg}}^{\min}) + \dot{H}_{\mathrm{cg}}^{\min}] \\ & + (1 - \mathbf{cg_{pw}}(t))[m_2^{\mathrm{gas}}(\dot{H}_{\mathrm{cg}}(t) - \dot{Q}_{\mathrm{cg,pw}}) \\ & + m_1^{\mathrm{gas}}(\dot{Q}_{\mathrm{cg,pw}} - \dot{Q}_{\mathrm{cg}}^{\min})],\end{aligned} \tag{16}$$

$$\mathbf{cg_{on}}(t)\in\{0, 1\}, \tag{17}$$

$$\mathbf{cg_{pw}}(t)\in\{0, 1\}, \tag{18}$$

$$\begin{aligned}\dot{Q}_{\mathrm{cg}^{\min}}\cdot\mathbf{cg_{on}}(t) \le \dot{Q}_{\mathrm{cg}}(t) \le {} & \dot{Q}_{\mathrm{cg}}^{\max}\cdot\mathbf{cg_{on}}(t) \\ & + \mathbf{cg_{start\text{-}up}}(t)\cdot\eta_{\mathrm{cg,th}}^{\text{start-up}}\cdot\dot{H}_{\mathrm{cg}}^{\max}\,\Delta t,\end{aligned} \tag{19}$$

$$\mathbf{cg_{start\text{-}up}}(t) \ge 0 \tag{20}$$

$$\mathbf{cg_{start\text{-}up}}(t) \ge \mathbf{cg_{on}}(t+\Delta t) - \mathbf{cg_{on}}(t) \tag{21}$$

$$\sum_{i=t+\Delta t}^{t+n_{\mathrm{cg,on}}^{\min}} \mathbf{cg_{on}}(i)\,\Delta t \ge \mathbf{cg_{start\text{-}up}}(t)\cdot n_{\mathrm{cg,on}}^{\min}, \tag{22}$$

$$\sum_{i=t_0}^{t_0+\tilde{n}_{\mathrm{cg,on}}^{\min}-\Delta t} \mathbf{cg_{on}}(i)\Delta t \ge \tilde{n}_{\mathrm{cg,on}}^{\min}. \tag{23}$$

Eqs. (15, (16) and (18) describe the piecewise approximation of the electrical output $\dot{E}_{\mathrm{cg}}$ and gas input $\dot{H}_{\mathrm{cg}}$ of the cogeneration unit as a function of the heat output $\dot{Q}_{\mathrm{cg}}$ (Fig. 2). These approximations

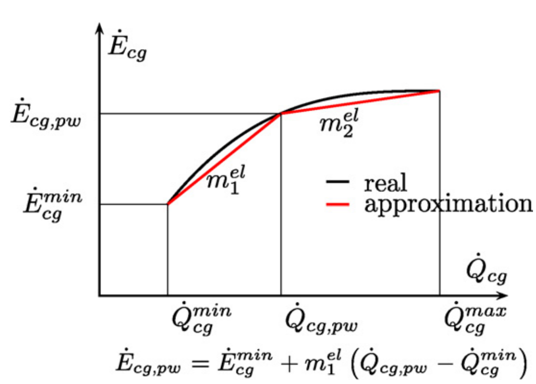

Fig. 2. Piecewise approximation schematics for the electrical output of the cogeneration unit as a function of the heat output. m_1^{el} and m_1^{el} are the slopes of the linear segments.

have been calculated using the efficiency charts provided by the manufacturer in Solo Stirling (2005), and converting the nominal power on these charts to the value given in Table 1 by a proportion rule.

The second term of the right hand side of Eqs. (15) and (16) as well as the last term of the upper bound of Eq. (19) are both derived from the assumption that during start-up, the cogeneration unit runs at full regime. However, most of the power is used to heat up the unit, and only a fraction of electrical output ($\mathbf{cg_{start\text{-}up}}(t)\cdot\eta_{\mathrm{cg,el}}^{\text{start-up}}\cdot\dot{H}_{\mathrm{cg}}^{\max}\Delta t$) and thermal output ($\mathbf{cg_{start\text{-}up}}(t)\cdot\eta_{\mathrm{cg,th}}^{\text{start-up}}\cdot\dot{H}_{\mathrm{cg}}^{\max}\,\Delta t$) is produced. These values have been calibrated using field tests of similar equipment (Ferguson, 2005; Knight & Ugursal, 2005).

Eqs. (20) and (21) define the variable $\mathbf{cg_{start\text{-}up}}(t)$ that has the value 1 at the times t when the cogeneration unit is started. Since it is related to integer variables, it only takes the values 0 or 1, but is defined as a real variable. Eq. (22) constrains the cogeneration unit to run for at least $n_{\mathrm{cg,on}}^{\min}$ hours.

Furthermore, $\tilde{n}_{\mathrm{cg,on}}^{\min}$ in Eq. (23) accounts for the hours the cogeneration unit sill has to operate from t_0 (if it was started less than $n_{\mathrm{cg,on}}^{\min}$ hours ago, $\tilde{n}_{\mathrm{cg,on}}^{\min} > 0$, otherwise $\tilde{n}_{\mathrm{cg,on}}^{\min} = 0$).

Domestic hot water tank:

$$Q_{\mathrm{dhw}}(t+\Delta t) = Q_{\mathrm{dhw}}(t) + (\dot{Q}_{\mathrm{dhw}}^{+}(t) - \dot{Q}_{\mathrm{dhw}}^{-}(t) - \dot{Q}_{\mathrm{dhw}}^{\mathrm{loss}}(t))\,\Delta t \tag{24}$$

$$\begin{aligned}\dot{Q}_{\mathrm{dhw}}^{\mathrm{loss}}(t) = {} & \frac{\pi}{(1/2\lambda)\log(D_{\mathrm{dhw}}/d_{\mathrm{dhw}}) + (1/\alpha_1 d_{\mathrm{dhw}}) + (1/\alpha_2 D_{\mathrm{dhw}})} \\ & \times h_{\mathrm{dhw}}(T_{\mathrm{dhw}}(t) - T_{\mathrm{dhw,room}}),\end{aligned} \tag{25}$$

$$T_{\mathrm{dhw}}(t) = \frac{Q_{\mathrm{dhw}}}{c_p V_{\mathrm{dhw}}} + T_{\mathrm{dhw}}^{\min} \tag{26}$$

$$0 \le \dot{Q}_{\mathrm{dhw}}(t) \le \dot{Q}_{\mathrm{dhw}}^{\max}. \tag{27}$$

Heat storage tank:

$$T_{\mathrm{hs}}(t+\Delta t) = T_{\mathrm{hs}}(t) + (\dot{Q}_{\mathrm{hs}}^{+}(t) - \dot{Q}_{\mathrm{hs}}^{-}(t) - \dot{Q}_{\mathrm{hs}}^{\mathrm{loss}}(t))\frac{\Delta t}{c_p V_{\mathrm{hs}}} \tag{28}$$

$$Q_{\mathrm{hs}}(t) = (T_{\mathrm{hs}}(t) - T_{\mathrm{hs}}^{\min}(t))c_p V_{\mathrm{hs}}, \tag{29}$$

$$\begin{aligned}\dot{Q}_{\mathrm{hs}}^{\mathrm{loss}}(t) = {} & \frac{\pi}{(1/2\lambda)\log(D_{\mathrm{hs}}/d_{\mathrm{hs}}) + (1/\alpha_1 d_{\mathrm{hs}}) + (1/\alpha_2 D_{\mathrm{hs}})} \\ & \times h_{\mathrm{hs}}(T_{\mathrm{hs}}(t) - T_{\mathrm{hs,room}}),\end{aligned} \tag{30}$$

$$\begin{aligned}T_{\mathrm{hs}}^{\min}(t) = {} & T_{\mathrm{h}}^{\min}(t) + \frac{\Delta T_0}{2} + \frac{T_{\mathrm{h}}^{\min}(t) - T^{\mathrm{ext}}(t)}{T_{\mathrm{h}}^{\min}(t) - T_0^{\mathrm{ext}}} \\ & + \left(\frac{T_0^{\min} - \Delta T_0}{2} - T_{\mathrm{h}}^{\min}\right)\left(\frac{T_{\mathrm{h}}^{\min}(t) - T^{\mathrm{ext}}}{T_0^{\min} - T_0^{\mathrm{ext}}}\right)^{1/q}\end{aligned} \tag{31}$$

$$0 \le \dot{Q}_{\mathrm{hs}}^{-}(t) \le \dot{Q}_{\mathrm{hs}}^{\max}\cdot T_{\mathrm{hs}}^{\min}(t) \le T_{\mathrm{hs}}(t) \le T_{\mathrm{hs}}^{\max}. \tag{32}$$

Eqs. (25) and (30) model the losses of the storage tanks according to Rietschel and Raiss (1973). Eq. (31) is used to calculate the minimal temperature required for the heat storage tank $T_{\mathrm{hs}}^{\min}$ according to the normalized equation from *Swiss Engineers and Architects Handbook* (norme SIA 384/2, 1988) applied to the nominal external temperature T_0^{ext} and the nominal heating water output temperature $T_0^{\min}$ (Zehnder, 2004).

For the storage tanks (heat and DHW), it has been assumed that the volume of the water contained in the storage tanks is constant, the temperatures are homogeneous, the mixture is instantaneous, and the losses from radiation are negligible.

Building temperature model:

$$T_h(t+2\Delta t_{sim}) = T_h^0(1+a_1+a_2) - a_1 T_h(t+\Delta t_{sim}) - a_2 T_h(t) + b_1 \dot{Q}_h^+(\tilde{t}) + b_2 \dot{Q}_h^+(t), \quad (33)$$

$$\dot{Q}_h^+(t) = \dot{Q}_{hs}^-(t) + \dot{Q}_{hs}^{gains}(t) - \dot{Q}_h^{loss}(t), \quad (34)$$

$$\dot{Q}_h^{gains}(t) = \dot{Q}_{sun}(t) + \dot{Q}_{vent}(t), \quad (35)$$

$$\dot{Q}_h^{loss}(t) = (T_h(t) - T^{ext})R_h \quad (36)$$

Eq. (33) is the second order model for the inside temperature of the building T_h. This model was estimated using an Auto Regressive eXternal inputs (ARX) method. The parameters a_1, a_2, b_1 and b_2 are estimated using the measurements of the system to be controlled. Note that it is the temperature difference $\Delta T(t) = T_h(t) - T_h^0$ that is modelled, thus the term $T_h^0(1+a_1+a_2)$. In this study $T_h^0 = 18\,^\circ C$.

In Eq. (33), Δt_{sim} is the building simulation time step, that is a fraction of or equal to Δt to have a better resolution of the building dynamics. Parameters a_1, a_2, b_1 and b_2 depend on this parameter.

In Eq. (34),

$$\tilde{t} = \begin{cases} t, & \text{if } t+\Delta t_{sim} < t+\Delta t \\ t+\Delta t, & \text{if } t+\Delta t_{sim} \geq t+\Delta t \end{cases},$$

since $\dot{Q}_{hs}^-(t)$ is constant during Δt, as well as the gains.

The three-way valve balance:

$$\dot{Q}_{cg}(t) + \dot{Q}_b(t) = \dot{Q}_{dhw}^+(t) + \dot{Q}_{hs}^+(t). \quad (37)$$

Eq. (37) comes from energy conservation, since there is no heat accumulation between the cogeneration unit, the boiler and the input of the storage tanks. Losses in the pipes are considered to be negligible.

The link equations:

$$\dot{E}_h^{req}(t) = \dot{E}_{cg}^{buy}(t) + \dot{E}_{el}^{buy}, \quad (38)$$

$$\dot{E}_{el}^{sell}(t) = \dot{E}_{cg}^{sell}, \quad (39)$$

$$\dot{E}_{cg}(t) = \dot{E}_{cg}^{buy} + \dot{E}_{cg}^{sell}, \quad (40)$$

$$\dot{Q}_{dhw}^{req}(t) = \dot{Q}_{dhw}^-(t). \quad (41)$$

The initial conditions, for the temperatures and energy storage tanks:

$$T_h(t_0) = T_{h,0}, \quad (42)$$

$$T_h(t_0 - \Delta t_{sim}) = T_{h,-1}, \quad (43)$$

$$T_h(t_0 - 2\Delta t_{sim}) = T_{h,-2}, \quad (44)$$

$$T_{hs}(t_0) = T_{hs,0}, \quad (45)$$

$$Q_{dhw}(t_0) = Q_{dhw,0}, \quad (46)$$

where the values $T_{h,0}$, $T_{hs,0}$, $Q_{dhw,0}$ correspond to the state of the system at t_0.

The cyclic constraints, for all variables$\mathbf{A_i}$:

$$\mathbf{A_i}(t_0+1+24) = \mathbf{A_i}(t_0+1), \quad (47)$$

Eq. (47) is added to so that the state of the system in the optimisation model should be recovered after 24 h of operation, by imposing that one day will resemble to the next. For instance, the storage tanks temperature should be similar at the same time every day.

However, the state of the system at t_0 may not be a "good" state, if it is outside the temperature comfort range, therefore, it is not reasonable to aim at attaining the same state after 24 h. It is however assumed that the system can recover to a "good" state (inside the comfort temperature range) within one hour. In consequence, the cycling is done between t_0+1 and t_0+1+24.

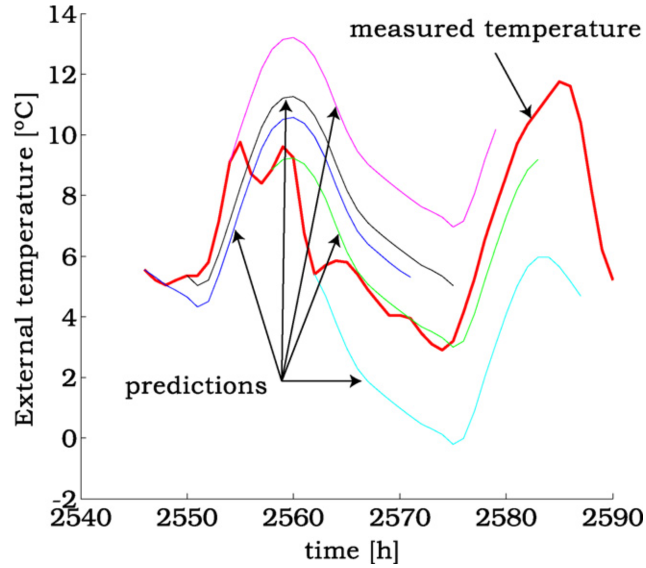

Fig. 3. Real and predicted external temperatures T^{ext} at different times t_0 (not consecutive).

3.2. Prediction

The optimal control strategy model requires four input parameters:

- The equipment and building characterisation parameters that define the performances of the technical equipment.
- The set points and market conditions that represent the energy services demand from the users such as comfort temperature at a given time of the day, hot water requirement, electricity prices, ...
- The measured variables that define the state of the system at a given time
- The predicted values that are needed to model the energy requirements for the next 25 h.

Parameters like the external temperature, the hot water consumption, electricity requirements, gains from inhabitants, electrical appliances and solar gains are unknown for $t > t_0$ and need to be predicted.

The outside temperatures $T^{ext}(t)$ for $t > t_0$ were predicted using the mean values of the variation of the temperature of the last 30 days (Henze, Kalz, Felsman, & Knabe, 2004). The estimated temperature rise between t_0 and $t_0+\Delta t$ is estimated by

$$T^{ext}(t_0+\Delta t) - T^{ext}(t_0) = \frac{1}{N}\sum_{n=1}^{N} T^{ext}(t_0+\Delta t-24n) - T^{ext}(t_0-24n) \quad (48)$$

therefore, for $N = 30$ and for $k = 1, 2, \ldots, \Delta t_{MH}/\Delta t$

$$T^{ext}(t_0+k\,\Delta t) = T^{ext}(t_0) + \frac{1}{30}\sum_{n=1}^{30} T^{ext}(t_0+k\,\Delta t-24n) - T^{ext}(t_0-24n) \quad (49)$$

here, the temperatures $T(t)$, for $t \leq t_0$, are known since they have been measured and stored.

Fig. 3 shows an example of the results obtained for the prediction of the external temperature using this technique. The figure shows that the predictions follow the general trend of the temperature profile.

The same prediction method is used to predict the energy requirements $\dot{E}_{\mathrm{h}}$ and $\dot{Q}_{\mathrm{dhw}}^{\mathrm{req}}$ as well as the solar gains $\dot{Q}_{\mathrm{sun}}$.

4. Validation

The predictive controller has been validated by testing the response of the control strategy using a dynamic building simulation model.

The procedure described in Sections 4.1 and 4.2 is repeated alternatively for $t_0 = t_{\mathrm{start}}, t_{\mathrm{start}} + \Delta t, \ldots, t_{\mathrm{end}}$. The resulting objective function and operating costs are calculated as shown in Section 4.3.

4.1. Optimisation

Giving an initial state of the system at t_0, the MILP problem presented in Section 3 is solved to find the optimal values of the decision variables $\mathbf{u}_{\mathrm{cg}}(t)$, $\mathbf{u}_{\mathrm{hs}}(t)$, $\mathbf{u}_{\mathrm{dhw}}(t)$ and $\mathbf{u}_{\mathrm{vlv}}(t)$ for $t_0 \le t \le t_0 + \Delta t_{\mathrm{MH}}$.

The optimal set-points resulting from this optimisation ($\mathbf{u}^*_{\mathrm{cg}}(t_0)$, $\mathbf{u}^*_{\mathrm{hs}}(t_0)$, $\mathbf{u}^*_{\mathrm{dhw}}(t_0)$ and $\mathbf{u}^*_{\mathrm{vlv}}(t_0)$) are applied to the detailed simulation model of the building and the energy conversion system in order to model the dynamic response of the system for the period t_0 to $t_0 + \Delta t$.

AMPL (Fourer, Gay, & Kernighan, 2003) was used for the mixed-integer linear programming, and solved using the CPLEX 9.0 solver (ILOG, 2003), which uses the branch and bound algorithm to solve the MILP problem.

4.2. Simulation

The set-points resulting from the optimisation ($\mathbf{u}^*_{\mathrm{cg}}(t_0)$, $\mathbf{u}^*_{\mathrm{hs}}(t_0)$, $\mathbf{u}^*_{\mathrm{dhw}}(t_0)$ and $\mathbf{u}^*_{\mathrm{vlv}}(t_0)$) are applied to the detailed simulation model of the building and the energy conversion system in order to model the dynamic response of the system for the period t_0 to $t_0 + \Delta t$.

The model is built using a Matlab/Simulink model of the building's thermal behavior adjusted to correspond to the SIA 380/1 target value single family home (Dorer et al., 2005), the heat distribution system and a non-linear cogeneration engine using the efficiency charts on Solo Stirling (2005).

Standard and stochastic profiles of outside temperature, solar gains, internal free gains, electricity consumption and DHW consumption were used to simulate the environment and the inhabitants' behavior. The simulation was done using the real values to validate the behavior of the control system when there are discrepancies between the predicted values and the observed values.

The discrepancies between the *predicted* and *real* values of the inputs and outputs of the cogeneration unit are taken into account and adjusted to calculate the *real* costs of operation (electricity bought and sold, gas consumption).

The storage tanks are simulated using the first order models described in Eqs. (24)–(27) for the domestic hot water tank, and Eqs. (28)–(32) for the heat storage tank in Section 3 without the boundary constraints for Q_{dhw} and T_{hs} (Eqs. (27) and (32)).

When the energy or temperature of the storage tanks is below the allowed range $Q_{\mathrm{dhw}} < 0$ or $T_{\mathrm{hs}} < T_{\mathrm{hs}}^{\min}$, the energy required for $Q = 0$ and $T_{\mathrm{hs}} = T_{\mathrm{hs}}^{\min}$ is produced by a backup boiler. This additional energy gives an estimation of the reserve needed for the storage tanks.

On the other hand, if these values are above the upper limit, $\dot{Q}_{\mathrm{dhw}} > \dot{Q}_{\mathrm{dhw}}^{\max}$ or $T_{\mathrm{hs}} > T_{\mathrm{hs}}^{\max}$ the additional energy is assumed to be evacuated and lost to the environment.

4.3. Optimal costs

The system performance costs $\tilde{\mathbf{J}}^*$ and $\tilde{\mathbf{C}}^*_{\mathrm{op}}$ for a given period $t_{\mathrm{start}} \le t \le t_{\mathrm{end}}$ are given by

$$\tilde{\mathbf{J}}^* = \sum_{t=t_{\mathrm{start}}}^{t_{\mathrm{end}}} \tilde{\mathbf{J}}(\mathbf{U}^*(t)) \tag{50}$$

and

$$\tilde{\mathbf{C}}^*_{\mathrm{op}} = \sum_{t=t_{\mathrm{start}}}^{t_{\mathrm{end}}} \tilde{\mathbf{C}}_{\mathrm{op}}(\mathbf{U}^*(t)) \tag{51}$$

$\tilde{\mathbf{J}}$ and the $\tilde{\mathbf{C}}_{\mathrm{op}}$ differ from that of Eqs. (1) and (3) because they take into account the *real* operating costs and penalties that result from the simulation model described in the previous section.

5. Results

The controller strategy and simulation was tested during five days in spring. In fact, this season is more interesting for validating the control strategy, because mild temperatures will result in more modulation of the cogeneration unit load charge. During summer, the cogeneration would stay off most of the time, since there is no need for space heating, and during winter it will run mostly at full power.

During the spring period, the operating costs for the system with the cogeneration unit are found to be 13% lower than the operating costs of the system using a boiler and importing the electricity from the grid and considering the same storage strategy.

Fig. 4 compares the room temperature T_{h} with its set-point and the temperature predicted by the controller for three non-consecutive strategy re-evaluation times. This picture shows that the controller re-evaluates the strategy and adapts it at every time interval allowing it to compensate the perturbations and the inaccuracies of the predictions.

Fig. 5 illustrates the behavior of the controller when the energy stored in the domestic hot water tank is not sufficient to fulfill the

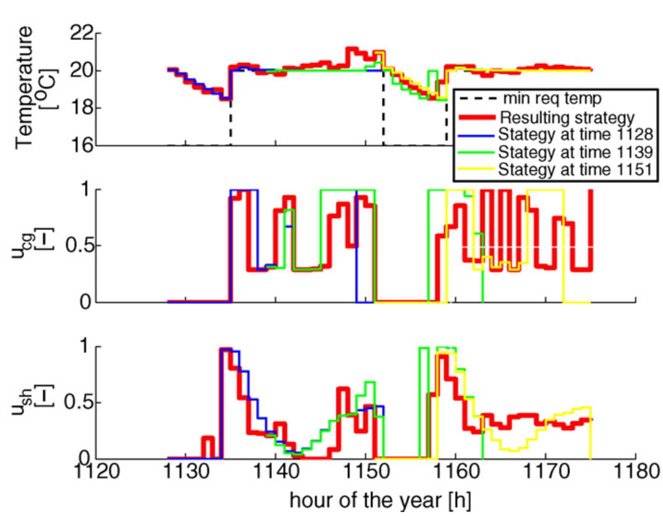

Fig. 4. Resulting and predicted strategies for the room temperature, cogeneration unit load charge and heat storage tank load charge for different times (not consecutive).

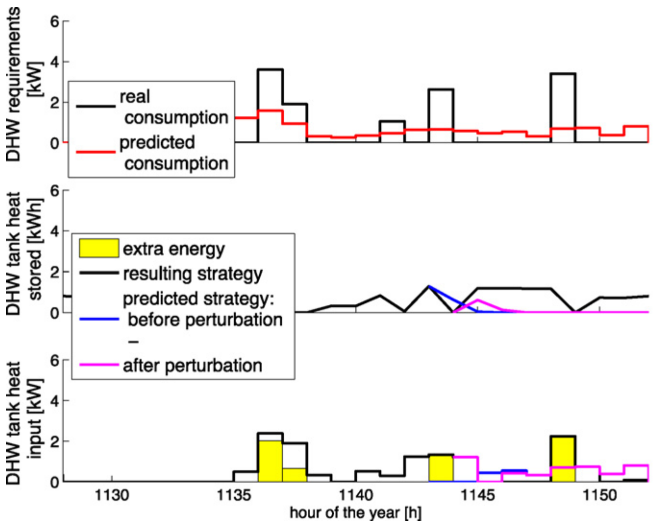

Fig. 5. Resulting and predicted strategies for domestic hot water tank.

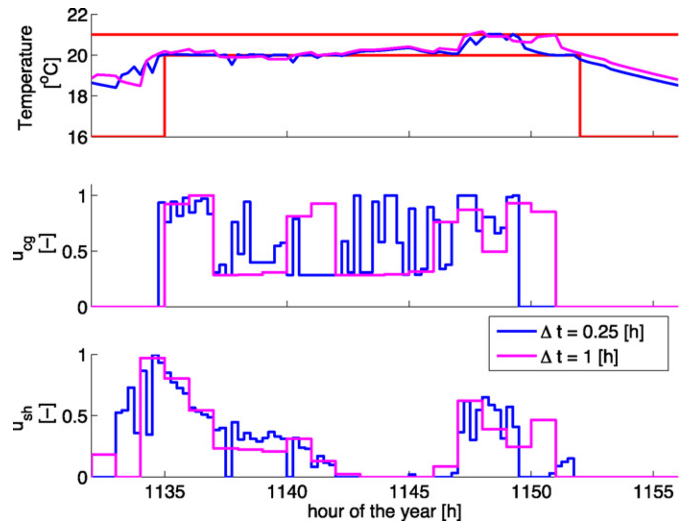

Fig. 7. Inside temperature T_h, cogeneration unit load charge $\mathbf{u}_{cg}$ and the heat storage tank load charge $\mathbf{u}_{hs}$ for different time sampling intervals.

requirements. This is the case because the prediction method used results in a flat and long domestic hot water consumption from 1135 to 1150, while, the real consumption presents a peak between 1136 and 1138 resulting in a consumption that will empty the tank. In these cases, the energy required is accounted as if it was produced by the backup boiler.

Fig. 6 illustrates the controller performance when the predictions of the inside temperature T_h differ from the real one and the temperature goes below the required temperature. In such a case, the strategy is adapted automatically in order to reach the comfort temperature set-point as quickly as possible. As Fig. 6 shows, the strategies for the $\mathbf{u}_{cg}$, and $\mathbf{u}_{hs}$ are adapted in order to produce more heat and increase the amount of heat that is delivered for space heating.

5.1. Analysis of the strategy re-evaluation frequency

Fig. 7 shows the results for calculations with a different value for Δt. For $\Delta t = 0.25$ [h] the strategy modulates considerably more than when the strategy is re-evaluated every hour. This may not be an advantage in real applications. Moreover, as the figure shows, there is not a considerable difference on the general aspect of the resulting inside temperature or on the strategy for $\mathbf{u}_{hs}$.

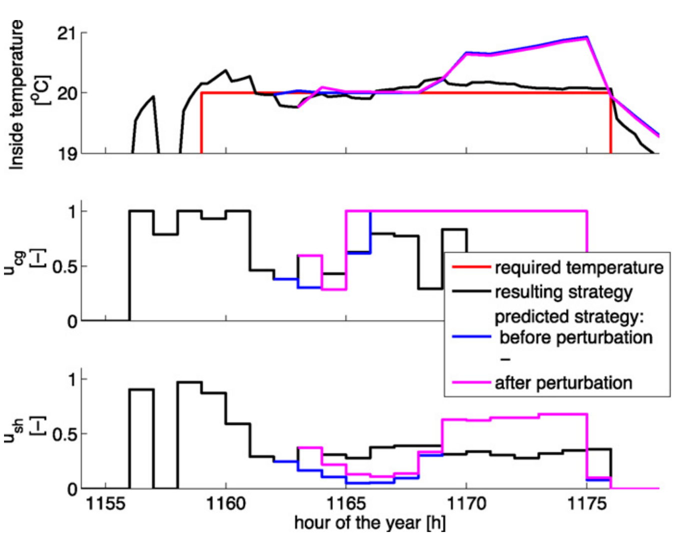

Fig. 6. Resulting and predicted strategies for the building inside temperature.

Table 2
Operating costs $\tilde{\mathbf{C}}^*_{op}$ and cost function value $\tilde{\mathbf{J}}^*$ as well as calculation time Δt_{calc} for time steps $\Delta t = 0.25$ [h] and $\Delta t = 1$ [h]. Simulation for 5 days in spring (starting at day 46). Horizon length $\Delta t_{MH} = 24$ [h].

	Δt	
	0.25 [h]	1 [h]
$\tilde{\mathbf{C}}^*_{op}$ [euro]	29.11	28.33
$\tilde{\mathbf{J}}^* \times 10^{-6}$	1.24	2.49

As Table 2 shows, the resulting strategy for $\Delta t = 0.25$ [h] has a lower cumulative value of the resulting objective function $\tilde{\mathbf{J}}^*$, since the strategy is re-evaluated at shorter intervals and can compensate earlier for prediction and model imprecisions.

For $\Delta t = 0.25$, higher operating costs are obtained since comfort is the priority of the control strategy. Furthermore, for $\Delta t = 0.25$ [h], more calculation time is required. In fact, the size of the problem (in particular integer variables) and the number of strategy calculations are multiplied by a factor 4. Table 3 compares the computing time for $\Delta t = 1$ h and $\Delta t = 15$ min. When $\Delta t = 1$ h the calculation time is very small.

In average, the time for writing files, simulation and communication between Matlab and AMPL corresponds to 1.3 s per iteration (not included in the values shown in Table 3). This time is independent from the re-evaluation time Δt. In real applications, this will correspond to reading and storing the acquired data from the sensors and the database.

This shows that it would be possible to centralize the calculation of the strategies in a single calculation unit that will send the

Table 3
Size of the problem (number of variables and constraints) and mean, maximum and minimum calculation times Δt_{calc} per optimisation for different re-evaluation times Δt.

	Time step Δt in [h]	
	0.25	1
Variables (total)	4560	1176
Binary	192	48
Constraints	3879	999
Mean Δt_{calc} [s]	16.98	0.30
max Δt_{calc} [s]	91.27	0.54
min Δt_{calc} [s]	0.50	0.04

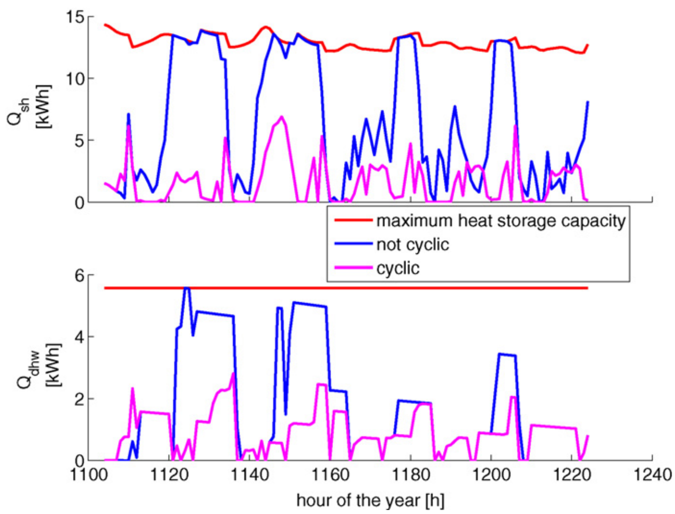

Fig. 8. Energy stored in the storage tanks with and without the cyclic horizon approach.

strategies to many buildings, instead of a local calculation unit for each building, that will only work for a fraction of a second every hour.

5.2. Cyclic model analysis

Fig. 8 compares the energy management with and without the cyclic constraint (Eq. (47)).

Two horizon lengths have been considered, $\Delta t_{MH} = 24\,[\mathrm{h}]$ for an *open* horizon and $\Delta t_{MH} = 25\,[\mathrm{h}]$ for a *cyclic* horizon.

The strategy that uses the cyclic constraint features a better management of the storage tanks avoiding to store heat in the tanks for longer periods and therefore reducing the storage losses. Table 4 shows that the operating costs for the cyclic strategy are 2% lower with no additional penalty on the comfort or in the reserve energy required.

Fig. 8 shows that for the storage tanks, the cyclic control strategy stores less energy, resulting in a more *borderline* control strategy.

5.3. Considering variable electricity market price

In the Virtual Power Plants perspective (Management Summary Report of EU-Project No. NNE5-2000-208, 2005), the case where the electricity price is not constant has been assessed to demonstrate the capabilities of the controller to adapt the strategy in order to take advantage of a time dependent electricity price. The controller was used from *the electricity provider point of view* using either a constant or a time dependent electricity price and assuming that the price for the electricity is the same for incoming and outgoing electricity (assuming 6% grid losses).

Fig. 9 compares the strategies with a varying electricity price and a constant electricity price on a regular day. The varying price

Table 4
Operating costs $\tilde{\mathbf{C}}^*_{op}$ and objective function value $\tilde{\mathbf{J}}^*$, and maximum additional energy required for *cyclic* and *open* strategies. Simulation for 5 days in spring (starting at day 46).

	Not cyclic $\Delta t_{MH} = 24\,[\mathrm{h}]$	Cyclic $\Delta t_{MH} = 25\,[\mathrm{h}]$
$\tilde{\mathbf{C}}^*_{op}$ [euro]	28.33	27.82
$\tilde{\mathbf{J}}^* \times 10^{-6}$	2.49	2.11
$\max\{\dot{Q}^{add}_{dhw}\}$ [kW]	3.06	3.06
$\max\{\dot{Q}^{add}_{hs}\}$ [kW]	0.24	0.25

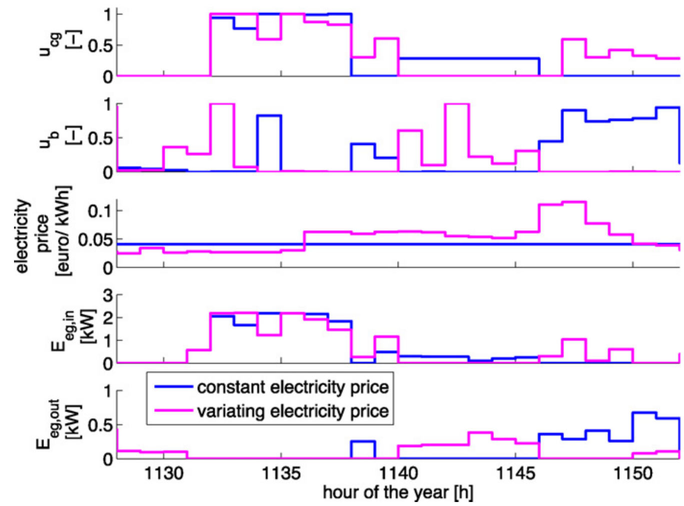

Fig. 9. Constant and time dependent electricity price. Regular day.

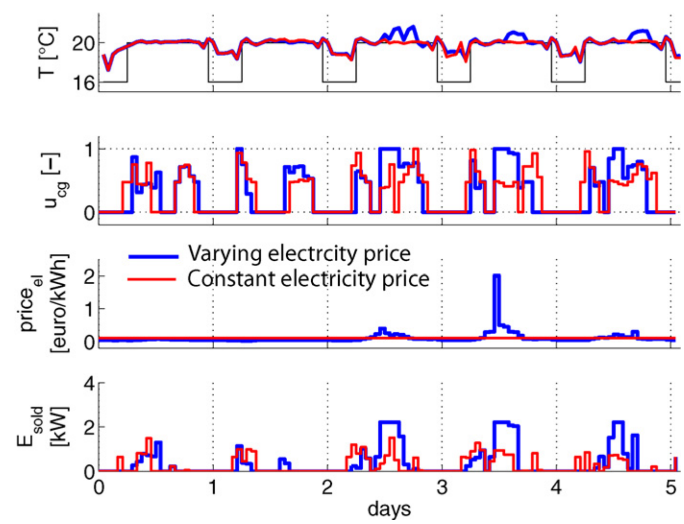

Fig. 10. Constant and time dependent electricity price. Extreme day.

reduces the cost of energy supply by 5% with no additional comfort violation.

Fig. 10 illustrates the control strategies in a day where the electricity has a very high peak. In this case, operating costs reduction can be 30%.

Both figures illustrate how the controller adapts the strategy to take advantage of higher electricity prices. In fact, when the price of electricity varies, the cogeneration unit is first stopped in order to empty the storage tank before starting cogenerating heat and electricity when the price is high. When considering the temperature in the room, one can observe that the controller even used the heat capacity of the building to maximize the cogeneration profit.

The time dependent prices were taken from the European Energy Exchange website[1], and the constant electricity price was the arithmetic mean of the time dependent electricity price over the time studied.

6. Conclusions

A model based predictive controller has been developed using a Mixed Linear and Integer Programming model to define the optimal

[1] http://www.eex.com.

management strategy of micro-cogeneration systems in building applications. The MILP model takes into account starting and shutdown of the unit as well as the partial load efficiency using a piecewise formulation. The model includes the balance of the hot water storage tanks as well as the heat accumulation in the building envelope.

The controller was validated with a numerical model of the system that is more detailed than the model used for the predictive controller.

The predictions of temperature and solar gains as well as the consumption of domestic hot water and electricity are obtained.

The *cyclic* horizon strategy has proved to deliver a better performance than the *open* horizon strategy.

In the virtual power plants perspective, this controller shows an ability to adapt the strategy in order to profit from fluctuating price of the electricity.

References

Arigiriou, A., Bellas-Velidis, I., & Balaras, C. (2000). Development of a neural network heating controller for solar buildings. *Neural Networks*, *13*, 811–820.

Dorer, V., Weber, R., & Weber, A. (2005). Performance assessment of fuel cell micro-cogeneration systems for residential buildings. *Energy and Buildings*, *37*, 1132–1146.

Entchev, E. (2003). Residential fuel cell energy systems performance optimization using “soft computing” techniques. *Journal of Power Sources*, *118*, 212–217.

Entchev, E., Gusdorf, J., Swinton, M., Bell, M., Szadkowski, F., & Kalbfleisch, W. (2004). Micro-generation technology assessment for housing technology. *Energy and Buildings*, *36*, 925–931.

Ferguson, A. (2005). *Model Specifications for Stirling-cycle based cogeneration device*. IEA/ACBCS Annex 42 Subtask B working Document.

Fourer, R., Gay, D., & Kernighan, B. (2003). *AMPL a modeling language for mathematical programming*. USA: Brooks/Cole-Thomson Learning.

Guillemin, A. (2003). Using genetic algorithms to take into account user wishes in an advanced building control system, *Ph.D. thesis*, École Polytechnique Fédérale de Lausanne.

Güntensperger, W., Haas, M., Lehmann, A., Renggli, B., & Tödtli, F. (2005). Control of concrete core conditioning systems. In *8th world congress for building technologies-CLIMA*

Gwerder, M., & Tödtli, J. (2005). Predictive control for integrated room automation. In *8th world congress for building technologies-CLIMA*.

Henze, G., Kalz, D., Felsman, C., & Knabe, G. (2004). Impact of Forecasting Accuracy on Predictive Optimal Control of Active and Passive Building Thermal Storage Inventory. *HVAC & R Research*, *10*(2), 153–178.

ILOG S.A., ILOG AMPL CPLEX System Version 9.0 User’s Guide (2003).

Knight, I., Ugursal, V. (2005). *Residential cogeneration systems: a review of the current technologies*. IEA/ACBCS Annex 42 Subtask A report.

Lamon, R., Gähler, C., Gwerder, M. (2007). Optimal Control of CHP Building Energy Systems, In *9th REHVA world congress for building technologies-CLIMA 2007*. Helsinki, 10th–14th June 2007.

Laubacher, N. (2006) Regelungsstrategien für ein Sirling-Mikro-Blockheizkraftwerk. *Master thesis*. ETHZ. Carried out at Siemens Building Technologies, HVAC products division.

Leyland, G. (2002). Multi-objective optimisation applied to industrial energy problems. *Ph.D. thesis*. Lausanne, Switzerland: EPFL.

Management Summary Report of EU-Project No. NNE5–2000-208 virtual fuel cell power plant; system-development, build, field installation and European demonstration of a virtual fuel cell power plant, consisting of residential micro-CHPs, 2005. Download under: ec.europa.eu/energy/res/sectors/doc/polygeneration/euvpp.pdf (08.04.2008).

Morel, N., Bauer, M., El-Khoury, M., & Krauss, J. (2001). Neurobat, a predictive and adaptive heating control system using artificial neural networks. *International Journal of Solar Energy*, *21*, 161–201.

Nygard-Ferguson, A. (1990). Predictive thermal control of building systems. *Ph.D. thesis*. École Polytechnique Fédérale de Lausanne.

Pearce, J., Zahawi, B., Awckland, D., & Starr, F. (1996). Electricity generation in the home: evaluation of single-house domestic combined heat and power. *Science Measurements and Technology*, *145*(6), 197–203.

Pearce, J., Zahawi, B., & Shuttleworth, R. (2001). Electricity generation in the home: modelling of single-house domestic combined heat and power. *Science Measurements and Technology*, *148*(5), 345–350.

Prud’Homme, T. (2002). Commande optimale d’une classe de systèmes hybrides: application aux kits solaires de production d’eau chaude sanitaire. *Ph.D. thesis*. École Polytechnique Fédérale de Lausanne.

Rietschel, H., & Raiss, W. (1973–1974). *Traité de chauffage et de climatisation*. Paris: Dunod.

Norme SIA 384/2: puissance thermique à installer dans les bâtiments. Société suisse ingénieurs et des architectes, 1988.

Solo Stirling 161 combined power heat (chp) module (2005).

Weber, C., Maréchal, F., Favrat, D., & Kraines, S. (2006). Optimization of an SOFC-based decentralized polygeneration system for providing energy services in an office-building in Tokyo. *Applied Thermal Engineering*, *26*(13), 1409–1419.

Zehnder, M. (2004). Efficient air–water heat pumps for high temperature lift residential heating, including oil migration aspects. *Ph.D. thesis*. École Polytechnique Fédérale de Lausanne.